

Melting of Submonolayer Krypton Films on Graphite

P. M. Horn,^(a) R. J. Birgeneau, P. Heiney, and E. M. Hammonds

Department of Physics, Massachusetts Institute of Technology, Cambridge, Massachusetts 02139

(Received 7 July 1978)

We present the results of a detailed x-ray scattering study of submonolayer krypton films physisorbed onto basal-plane surfaces of exfoliated ZYX graphite. Results illustrate that x-ray scattering may provide precise structural information about the solid and liquid phases of adsorbed films. For near-monolayer coverages, melting of the commensurate krypton solid appears to be a second-order transition with a critical exponent β consistent with a Potts lattice-gas model of the melting process.

Atoms and molecules physisorbed onto solid surfaces can exist in a variety of thermodynamic phases.^{1,2} In the submonolayer region, two-dimensional (2D) gas, liquid, and solid phases have been identified. Furthermore, the solid phase can be either commensurate or incommensurate with the underlying substrate surface.^{3,4} The transitions between these various two-dimensional phases are of considerable current theoretical and experimental interest. The solid-liquid transition is of particular importance because it can in principle be second order at high coverages and thus represents a 2D analog of the usual melting process which is first order in all known three-dimensional systems. In this paper, we present the results of an x-ray scattering study of the melting of submonolayer krypton films adsorbed onto basal-plane surfaces of exfoliated ZYX graphite.

The probable empirical phase diagram^{2,5} for krypton adsorbed on basal-plane surfaces of exfoliated graphite in the submonolayer, commensurate-structure range is schematically illustrated in Fig. 1. At low fixed coverages, the transition from fluid to solid is believed to be first order and two-phase coexistence obtains at low temperatures. Thermodynamic measurements⁵ suggest that near monolayer coverages, the liquid-solid transition may be second order so that at intermediate temperatures one has a single-phase crystalline krypton film. Theoretical models of the melting process depend strongly on the matching of the adsorbate-adsorbate, interaction potential with the underlying graphite lattice.² A Potts lattice-gas (PLG) model with nearest-neighbor exclusion has been developed to explain the phase diagram shown in Fig. 1.² This theory predicts a phase diagram which contains a line of second-order transitions at high coverages terminating at a multicritical point. Because of the hexagonal symmetry of the (001) surface of graphite, there are three equivalent sublattices within which the krypton can order.

Thus the predicted second-order transitions belong to the universality class of the 2D three-state Potts model.² The phase diagram predicted by the PLG model appears to be in reasonable agreement with the experimental data illustrated in Fig. 1.² The theory also makes detailed predictions for the critical behavior along the second-order line and at the multicritical point; none of these predictions has yet been tested experimentally. Clearly, therefore, krypton on graphite represents a very attractive system for studies of 2D melting.

The experiments were carried out on a two-axis x-ray spectrometer with the use of Cu $K\alpha$ radiation from a Rigaku 12-kW rotating-anode source. A parallel beam was obtained with a vertically bent pyrolytic-graphite monochromator. The beam was collimated horizontally via vertical slits before and Soller slits after the sample. In these experiments we used exfoliated ZYX graphite as a substrate⁶; ZYX graphite was chosen both because of its large (001) surface area and because of the enhanced preferential orientation of the (001) planes, compared with, for example, Grafoil.¹ The graphite was cut into strips 1.2 cm \times 1.7 mm \times 1 mm and these strips

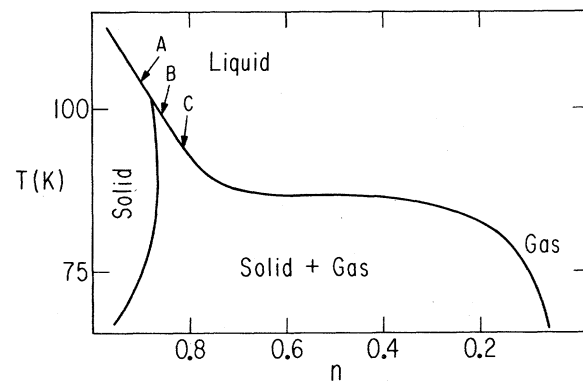


FIG. 1. Empirical phase diagram for submonolayer krypton on graphite as deduced from data in Ref. 5.

were carefully stacked to yield a well-aligned sample $1.2 \text{ cm} \times 1.2 \text{ cm} \times 1 \text{ mm}$ with the c axis in the vertical direction. The experiments were carried out in transmission through the 1-mm direction. This particular sample geometry was chosen so as to allow access of the x-ray beam to the entire sample; the cross section of the x-ray beam was typically 1.5 mm (horizontal) by 7 mm (vertical). This translates into an illuminated accessible surface area of about 20 cm^2 .

The gas handling system, baking of the graphite, cryostat systems, etc., all involved standard techniques.^{1,4,5} In general, our vapor pressure measurements agree with more detailed studies carried out previously⁵; however, because of our extremely small net surface area the absolute coverage is only known to about 5% although relative coverages are known rather more accurately. In this paper we adopt the approach of combining our accurate temperature measurements with the results from previous thermodynamic studies⁵ to estimate the scale factor for the coverage. Although there may be subtle differences between various graphite substrates we expect, nevertheless, that this procedure will be adequate for all of the results discussed here. The experiments were carried out in the closed-cell configuration, that is, the cell was filled with krypton until a given coverage near T_c was obtained and the sample cell was then closed off. Hence, as a function of temperature the coverage changed slightly, albeit in a known way. Limited data were also obtained at fixed temperature as a function of coverage with results consistent with the closed-cell measurements which span the predicted multicritical point. The coverages and approach to the liquid-solid phase transition are indicated by the arrows in Fig. 1.

The results of typical longitudinal scans are shown in Fig. 2 where we display two Bragg peaks of the ordered krypton solid. The graphite thermal diffuse background, which was typically about 12.5×10^3 counts/min for $q \cong 1.70 \text{ \AA}^{-1}$, was determined during clean-surface scans and was subtracted from the data in Fig. 2. The position of these and higher-order Bragg peaks unequivocally confirms that the krypton lattice structure is the $\sqrt{3} \times \sqrt{3}$ triangular lattice, commensurate with the graphite surface. The strength and narrowness of these peaks, when compared with, for example, neutron-scattering results for argon on Grafoil,⁴ illustrate the power of x-ray scattering as a probe of solid surfaces. The asymmetric shape of the Bragg peaks in Fig. 1 is typical of

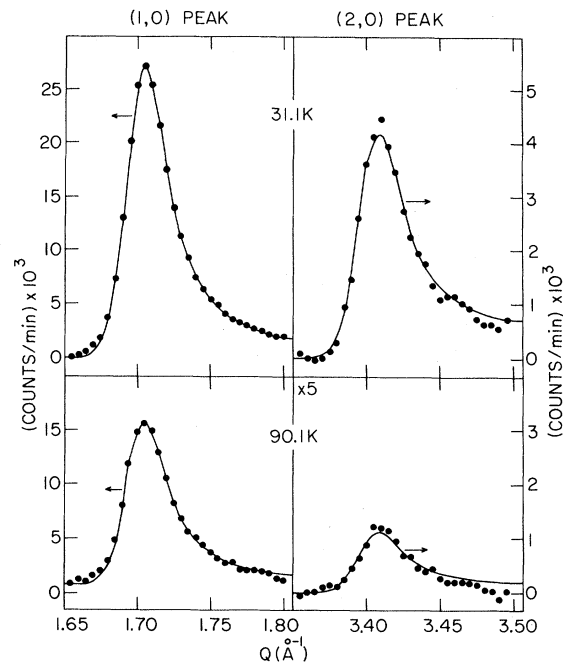


FIG. 2. X-ray scans of the (1,0) and (2,0) krypton peaks with the graphite background subtracted off. The solid lines represent the fitted Warren line shape as discussed in the text.

those observed in two-dimensional materials with a mosaic distribution of plane orientations. In order to fit these peaks we have used the standard theory of Warren⁷ for diffraction from 2D finite-size crystals together with the vertical-mosaic correction introduced by Kjems *et al.*⁴ A typical fit of the Warren theory to the low-temperature (1,0) peak is shown in the upper left of Fig. 2. The values of the relevant parameters are vertical mosaic = 11° [HWHM (half-width at half-maximum)], $q_0 = 1.700 \text{ \AA}^{-1}$, and mean particle size $L = 450 \pm 75 \text{ \AA}$. These same parameters were then used to calculate the (2,0) line shape shown in Fig. 2. Our measured value for L is consistent with estimates from specific heat measurements of helium on ZYX graphite by Bretz.⁶

As the melting transition is approached from below, the intensity of the Bragg peak decreases; simultaneously broad liquidlike scattering appears centered around $q_0 = 1.70 \text{ \AA}^{-1}$. This liquidlike scattering can be either static or dynamic in origin, the former arising from liquid-solid coexistence, the latter arising from dynamical fluctuations into the liquid state (critical scattering). As illustrated in the bottom left panel of Fig. 2, the solid portion of the (1,0) composite line can be fitted with the same size parameter used to de-

scribe the low-temperature data, implying that the size of the krypton crystals does not decrease appreciably as melting is approached. This, in itself, is an interesting result which we do not fully understand. The relative decrease in the size of the (2, 0) peak compared to the (1, 0) peak as the temperature is raised is a result of the temperature dependence of the Debye-Waller factor. These data in Fig. 2 imply a mean-square amplitude for the fluctuations of the krypton atoms about their equilibrium position of 0.055 \AA^2 at about 30 K increasing to approximately 0.17 \AA^2 at 90 K.

Because of the invariance of the line shape and position (and hence commensurability) of the (1, 0) peak with temperature, the peak intensity may be used directly to determine the total solid scattering as a function of temperature. In Fig. 3 we plot the peak intensity minus the intensity at the forward wing of the scattering, $I(q=1.706 \text{ \AA}^{-1}) - I(q=1.650 \text{ \AA}^{-1})$ for the three scans illustrated in Fig. 1. Since the scattering at $q=1.650 \text{ \AA}^{-1}$ is solely due to the liquid background, this subtraction procedure provides a rather good determination of the strength of the solid scattering alone. Let us now discuss each of the scans in succession. Scans B and C are essentially identical except for the shift in the phase-boundary temperature (T_c). Both most likely lie in the first-order region. In this case the (1, 0) peak intensity measures the amount of solid present. As the temperature is increased near T_c the solid signal decreases linearly with temperature while the coexisting liquid signal (not shown explicitly here) concomitantly increases. The explicit shape of scans B and C is consistent with the steep, nearly linear shape of the solid-liquid phase boundaries for $T \geq 85 \text{ K}$ as exhibited in Fig. 1. For scan B the correlation length of the liquid at T_c is $\sim 12 \text{ \AA}$. As the coverage is increased slightly (scan A) there is a drastic change in the krypton melting curve; this may be seen most clearly from the data near T_c (bottom part of Fig. 3). The data look very much like a smeared second-order transition as observed, for example, in certain 2D magnetic systems.⁸ Accordingly, we have fitted the intensity by a power law $I \sim \{T_c - T\}/T_c\}^{2\beta}$ convoluted with a Gaussian distribution of T_c 's. The explicit values obtained from these fits depend somewhat on the range of data included. We find as an average for scan A, $\beta = 0.09 \pm 0.03$, $\langle T_c \rangle = 105.87 \text{ K}$, and a Gaussian HWHM smearing $\sigma = 0.4 \text{ K}$. The value of $\sigma/\langle T_c \rangle = 0.004$ is consistent with the rounding observed in specific heat

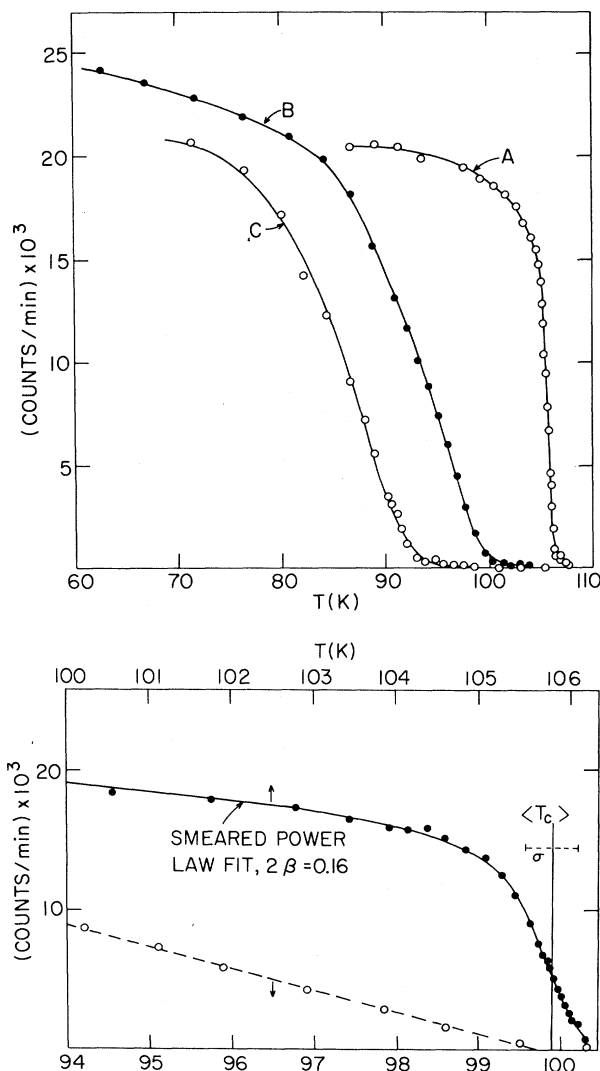


FIG. 3. Upper panel: (1, 0) peak intensity vs temperature for scans A, B, and C of Fig. 1. The solid lines are guides to the eye. The turnover at $\sim 90 \text{ K}$ for scan A is due to an incipient commensurate-incommensurate transition. Lower panel: blowup of region near T_c for scans A and B. The dashed line for scan B is a guide to the eye. The solid line for scan A is the result of a least-squares fit of a smeared power law to the data shown.

measurements of He on ZYX graphite.⁶ We note also that Ferdinand and Fisher,⁹ for the finite-size 2D Ising model, infer a rounding $\Delta T/T_c$ of $\sim 1/n$ where n is the number of sites along the number of sites along the side of a 2D array. In our case $n \approx 100$ so that clearly our fitted value for the rounding $\Delta T/T_c \approx 2\sigma/T_c = 0.008$ is consistent with the Ferdinand-Fisher result. Finally,

we note that Berker, Ostlund, and Putnam predict $\beta=0.10$ for their PLG model compared with our $\beta=0.09 \pm 0.03$.

To conclude, we reiterate the fact that these experiments have illustrated that x rays, in spite of their lack of surface selectivity, may provide extremely detailed information about surface film melting. Our experiments provide strong support for the PLG model of commensurate krypton on graphite, including the crossover from first- to second-order melting. However, primarily because of finite-size effects, we have only been able to demonstrate consistency rather than uniqueness. Critical liquid scattering measurements should be able to resolve the remaining ambiguities. Our initial data suggest that such measurements are indeed within the scope of an x-ray experiment and we anticipate results in the near future.

This work was supported by the Joint Services Electronics Program under Contract No. DAAG-29-78-C-0020.

^(a)Permanent address: James Franck Institute, University of Chicago, Chicago, Ill. 60637.

¹For a comprehensive review see J. G. Dash, *Films on Solid Surfaces* (Academic, New York, 1978).

²A. N. Berker, S. Ostlund, and F. A. Putnam, *Phys. Rev. B* **17**, 3650 (1978), and references therein.

³M. D. Chinn and S. C. Fain, Jr., *Phys. Rev. Lett.* **39**, 146 (1977).

⁴J. K. Kjems, L. Passell, H. Taub, J. G. Dash, and A. D. Novaco, *Phys. Rev. B* **13**, 1446 (1976); H. Taub, K. Carneiro, J. K. Kjems, L. Passell, and J. P. McTague, *Phys. Rev. B* **16**, 4551 (1977).

⁵A. Thomy and X. Duval, *J. Chim. Phys.* **66**, 1966 (1969), and **67**, 286, 1101 (1970); F. A. Putnam and T. Fort, Jr., *J. Phys. Chem.* **79**, 459 (1975), and **81**, 2164 (1977); Y. Larher, *J. Chem. Soc. Faraday Trans.* **70**, 320 (1974); G. A. Stewart and D. Butler, unpublished.

⁶M. Bretz, *Phys. Rev. Lett.* **38**, 501 (1977).

⁷B. E. Warren, *Phys. Rev.* **59**, 693 (1941).

⁸R. J. Birgeneau, J. Als-Nielsen, and G. Shirane, *Phys. Rev. B* **16**, 280 (1977).

⁹A. E. Ferdinand and M. E. Fisher, *Phys. Rev.* **185**, 832 (1969).

Dynamics of an Ising-like Model in Four Space Dimensions

T. Schneider and E. Stoll

IBM Zurich Research Laboratory, 8803 Rüschlikon, Zurich, Switzerland

(Received 7 July 1978)

Using a molecular-dynamics technique, we studied the excitation spectrum of an Ising-like lattice-dynamic model in four space dimensions. We found a central peak close to the transition temperature which does not evolve from the damped soft mode. Our results reveal that the overdamped-soft-mode picture and current interpretations of renormalization-group results for dynamic properties should be revised. They also provide testable predictions for Ising-like dipolar systems.

A recent development has been the application of renormalization-group techniques to dynamic critical phenomena.¹ As in the static case,² most calculations have been performed as an expansion in the parameter $\epsilon = 4 - d$, where d is the space dimension. For $d \geq 4$, the exponents for static critical phenomena are expected to be classical in most cases, and the conventional theory of critical slowing down¹ should hold. For an Ising-like system with dipolar forces, however, the static and dynamic critical properties will be classical for $d \geq 3$.^{2,3} The renormalization-group analysis also indicates that the critical dynamics of lattice-dynamic systems is equivalent to corresponding stochastic models with conserved energy.^{1,4} This has led to the conclusion that for lattice-dynamic systems with

short-range forces and $d \geq 4$, the dynamic critical behavior is associated with an overdamped soft mode. In particular, a sharp central peak around zero frequency, additional to a damped soft-mode resonance, should not occur in the spectral density of the order-parameter fluctuations.^{1,4} For Ising-like systems with dipolar forces these conclusions are expected to hold for $d \geq 3$.

The purpose of this Letter is to test these predictions by means of a molecular-dynamics technique, the conclusion being that the excitation spectrum of a four-dimensional Ising-like lattice-dynamic model with short-range forces differs, close to T_c , from the overdamped-soft-mode picture. This result does not imply that the critical slowing down is nonconventional. It reveals,